Coupling and competition between ferroelectric and antiferroelectric states in Ca-doped $Sr_{0.9-x}Ba_{0.1}Ca_xTiO_3$: Multipolar states

T. Wei
College of Science, Civil Aviation University of China, Tianjin 300300, China

J.-M. Liu*
Laboratory of Solid State Microstructures, Nanjing University, Nanjing 210093, China and International Center for Materials Physics, Chinese Academy of Sciences, Shenyang 110016, China

Q. J. Zhou and Q. G. Song
College of Science, Civil Aviation University of China, Tianjin 300300, China

(Received 29 September 2010; revised manuscript received 4 December 2010; published 4 February 2011)

We prepare a series of polycrystalline $Sr_{0.9-x}Ba_{0.1}Ca_xTiO_3$ (SBCT) with relatively low Ba- and Ca-doping levels, and their microstructural, ferroelectric, dielectric, and lattice dynamic properties are investigated. It is surprisingly found that a proper Ca^{2+} doping, which usually favors the antiferroelectric state in $SrTiO_3$, can remarkably enhance the ferroelectricity of SBCT. The coupling and competition between the ferroelectric state induced by Ba^{2+} doping and antiferroelectric state induced by Ca^{2+} doping lead to a sequence of multipolarized states, such as the enhanced polarization state, the cooperative polarization state, and the antiferroelectric state.

DOI: 10.1103/PhysRevB.83.052101 PACS number(s): 77.22.−d

$SrTiO_3$ (STO) is a peculiar and incipient ferroelectric (FE),[1–5] which displays a number of attractive new phenomena owing to the existence of quantum critical phenomena.[6,7] Because one of the triply degenerate R_{25} modes is frozen, the room-temperature (T) cubic perovskite structure transforms into a tetragonal phase below 105 K.[1–5] The dielectric permittivity (ε) of STO gradually increases on cooling and becomes nearly two orders of magnitude larger at $T \sim 10$ K, below which it levels off.[1–5] The quantum fluctuations (QFs) associated to a non-negligible zero-point energy suppress the onset of weak FE order. In spite of these features, STO is still very sensitive to dipole impurities, inducing complicated polarized states such as dipole glass, ferroglass, and FE state, etc.[8–12]

For example, the relatively low-level Ca^{2+} (ionic radius $r_{Ca} = 0.099$ nm) doping at the Sr^{2+} site can transform STO into an XY-type FE state[1] or ferrielectric and/or antiferroelectric (AFE) state.[13,14] Typical dielectric relaxor behavior was also observed in STO doped with small ions such as Bi^{3+} and Mn^{2+}.[15,16] On the other hand, for those STO systems doped with a large divalent ion such as Ba^{2+} ($r_{Ba} = 0.135$ nm) at the Sr^{2+} ($r_{Sr} = 0.112$ nm) site, a glasslike state, a relaxor state, and a normal FE state were identified with increasing doping level.[9] Interestingly, in this case, the favored state seems to be FE-like. It is understood that these small or large ion substitutions at Sr^{2+} site can induce remarkable lattice distortions, thus resulting in serious lattice mismatch between those doped regions and the surrounded STO host matrix. These lattice distortions can be simply characterized by the tolerance factor (TF) $t = (r_A + r_O)/\sqrt{2}(r_B + r_O)$, where r_A and r_B are the ionic size at sites A and B, and r_O is the size of the oxygen ion for an ABO_3 compound such as STO ($t = 1.01$). For small ion doping (e.g., Ca^{2+}), those doped regions show a smaller TF (e.g., $t = 0.97$) and off-center ion occupation, inducing elastic lattice strain. The as-generated off-center dipole moment ordering and corresponding reorientation dynamics are the major mechanisms responsible for the observed behaviors. Such an effect usually favors the AFE state, unless it is for cases of extremely low doping.

However, for large ion doping (e.g., Ba^{2+}), those doped regions have larger a TF than STO, and no off-center dipoles can form owing to the lattice mismatch between the regions with a large TF and a small TF. Instead, at low doping levels (e.g., ~10%), the quadrupole moments owing to the mismatch are developed and the quadrupole ordering into dipole domains would result in elastic lattice strains, too.[9,10] The interaction between these quadrupoles seems to be FE-like. In short, for STO, once the substitution is sufficiently high, both mechanisms (the off-center dipole ordering and quadrupole ordering) can respectively lead to various dipole-ordered states, such as $BaTiO_3$-dominant ferroelectrics or $CaTiO_3$-dominant AFEs. Therefore, the rich physics and fascinating phenomena in doped STO would lie mainly in the relatively low doping range.

While the two mechanisms mentioned above have been separately well understood, it is a proper time to address the potential competition and coupling between them (if any exist) in STO. Such coupling and competition may allow additional phenomena and physics to be discovered yet. A sober approach starts from the low-level Ba^{2+} and Ca^{2+} codoping in STO, where very different phenomena from those observed in individual Ba^{2+}- or Ca^{2+}-doped STO may be expected. More physics also lies in this approach. Taking low-level Ba^{2+}- (e.g., <10%) doped STO as an example, one observed glasslike or relaxorlike states associated with the quadrupole ordering,[9] while it is possible to drive this configuration into a normal FE state by properly doping Ca^{2+} ions, which in fact arises from the competition and coupling mentioned above, and thus leads to a remarkable enhancement of the FE property. This strategy will be demonstrated in this work, in addition to quite a few interesting effects.

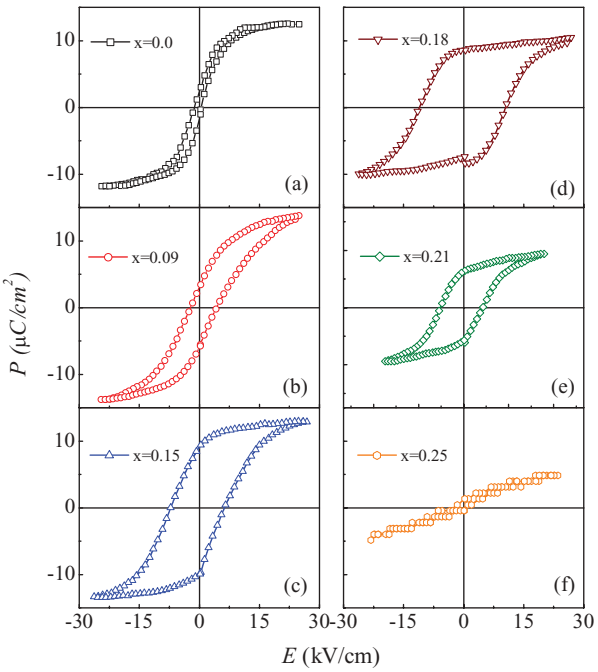

FIG. 1. (Color online) Measured P-E loops at $T = 10$ K for various samples with a Ca-doping level labeled in (a)–(f), respectively.

The experiment was performed by synthesizing a series of polycrystalline $Sr_{0.9-x}Ba_{0.1}Ca_xTiO_3$ (SBCT) samples by a solid-state reaction.[17] Note that the Ba doping here is low (10%) and insufficient to transfer STO into a normal FE state with well-defined polarization–electric field (P-E) hysteresis, even at low T. Then we look at the effect of Ca doping that is believed to favor the AFE state. X-ray diffraction (XRD) with Cu $K\alpha$ radiation indicated that all the samples have a perovskite structure at room temperature and no secondary phase was found. The FE was measured with an RT6000 FE tester from Radiant Technologies, Inc. in a standard mode with a pulse step rate of 4.0 ms. The dielectric permittivity ε as a function of T under a different ac signal frequency ($f = 1.0$, 10.0, and 100 kHz) was measured using an HP4294A impedance analyzer with a T sweeping rate of 2 K/min, both by inserting the samples into the Janis closed-cycle refrigerator system (Janis Research Company, Inc). To check the lattice dynamic of the samples at various T, the Raman spectroscopy was undertaken using a Renishaw inVia Raman microscope with an Ar-ion laser (514 nm) source.

Figure 1(a) presents the measured P-E loop for $x = 0$ at $T = 10$ K, where sample $x = 0$ ($Sr_{0.9}Ba_{0.1}TiO_3$) is believed to favor the FE state. It reveals that the Ba doping does suppress the QFs and induce FE behavior.[15,16] In this case, however, a serious polarization relaxation (PR) effect is identified, characterized by small remnant polarization (P_r) upon removal of electric field E although the saturated polarization (P_s) is large.[18] Microscopically, this PR effect implies that the FE domains associated with the quadrupole ordering are local and small in size and no macroscopic FE order is developed, obviously owing to the penalty of the elastic energy associated with the doping-induced lattice mismatch. What is interesting is that this serious PR effect can be suppressed substantially by Ca doping, as shown in Figs. 1(b) and 1(c), with x up to 0.15, where well-developed P-E loops with increasing P_r and coercivity E_c are observed. Further increasing x, however, results in the shrinking of both P_r and P_s. Eventually the hysteresis shrinks back to a thin loop with negligible P_r and E_c.

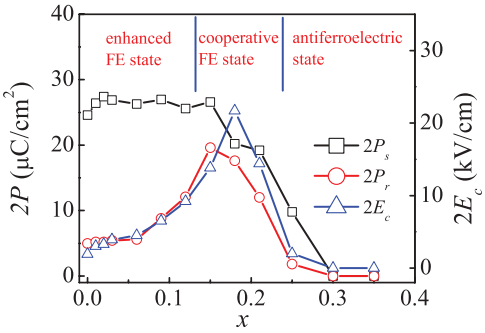

FIG. 2. (Color online) Dependences of measured $2P_s$, $2P_r$, and $2E_c$, on x at $T = 10$ K, with the three different polarization regions (enhanced FE state, cooperative FE state, and AFE state) separated by solid lines.

For a clearer illustration of the Ca-doping effect, we plot parameters P_s, P_r, and E_c as a function of x for all the samples in Fig. 2. The above-mentioned features can be reflected by three distinct regions. Roughly at $x < 0.15$, a gradual transition of the system from a FE state with a serious PR effect into a normal FE state with increasing x is observed, characterized by the well-developed P-E loop and rapidly increasing P_r and E_c. We refer to this region as the enhanced FE state. Roughly between $0.15 < x < 0.25$, one still observes well-developed P-E loops with P_r not much smaller than P_s, although P_s begins to decay with x at $x > 0.15$. This region can be referred to as the cooperative region, with the physics to be discussed below. As $x \sim 0.25$ and higher, no more of the P-E loop can be measured and an almost linear P-E dependence with $P_r \sim 0$ and $E_c \sim 0$ is found. This indicates that no more ferroelectricity is available. In fact, for such a high Ca-doping level, the off-center dipole ordering becomes dominant and the AFE state ensues, although the double-loop associated with the AFE state is not available to us owing to the extremely high E required at low $T = 10$ K.

The above experiments illustrate a clear fact that for the $Sr_{0.9}Ba_{0.1}TiO_3$, a system with a favored FE state, the Ca doping at the Sr site within a proper range does not suppress the FE but surprisingly enhances it. It is also shown that the Ca doping results in the appearance of multipolarized states, from an enhanced FE state to the cooperative "normal" FE state, and eventually to the AFE state.

To understand these multipolarized states in more convincing ways, we perform the dielectric and Raman spectroscopy measurements. In Fig. 3(a) we show the measured $\varepsilon(T)$ data under different frequencies f (1.0, 10.0, and 100 kHz) for samples $x = 0$, 0.15, and 0.21. For sample $x = 0$, a sharp dielectric anomaly at $T \sim 70$ K is observed, indicating the FE transitions. Moreover, Fig. 3(e) displays the Raman spectra for sample $x = 0$ at $T = 10$, 50, 70, 100, and 250 K, respectively. The strong first-order Raman peaks (single phonon) below the dielectric anomaly point (~70 K) can be detected. The Raman peaks at 174, 479, 549, and

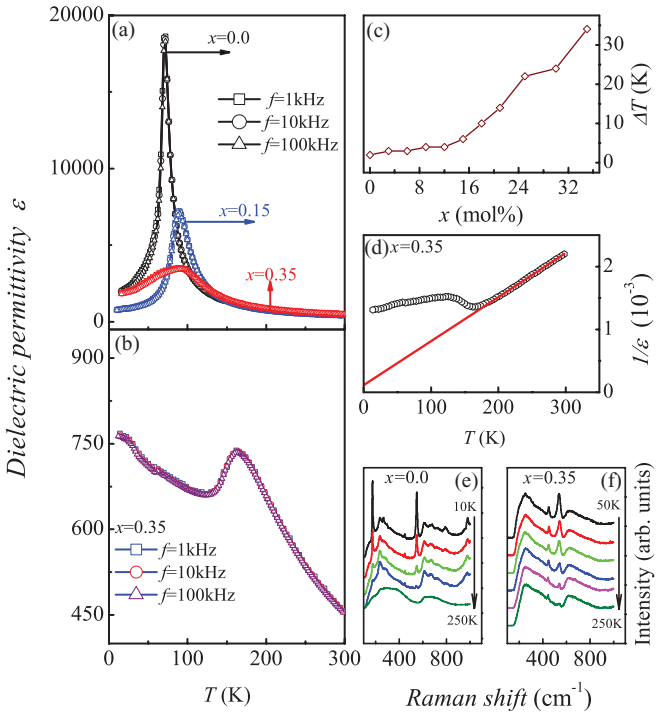

FIG. 3. (Color online) Measured ε as a function of T for samples $x = 0.0$, 0.15, 0.21 (a), and 0.35 (b), under frequency $f = 1.0$ kHz, 10.0, and 100 kHz, respectively. (c) Variation of evaluated ΔT with x. (d) The ε^{-1}-T plot for sample $x = 0.35$, and the solid line is the Curie-Weiss fitting result. (e) Measured Raman spectra for sample $x = 0.0$ at $T = 10$, 50, 70, 100, and 250 K, respectively. (f) Measured Raman spectra for sample $x = 0.35$ at $T = 50$, 75, 100, 150, 180, and 250 K, respectively.

792 cm^{-1}, correspond to the TO_2, LO_3, TO_4, and LO_4 phonons, respectively. Therefore, the dipole alignment in sample $x = 0$ at $T = 10$ K is already inside the FE state in spite of the thin P-E loop [Fig. 1(a)]. With increasing x, the dielectric peak is gradually broadened with the peak position shifting toward the high-T side and the peak height suppressed, indicating the enhanced dielectric smearing. As a quantitative measure, we evaluate $\Delta T = |T(0.9\varepsilon_{max}) - T(\varepsilon_{max})|$, as a function of x, where ε_{max} is the dielectric peak value, $T(0.9\varepsilon_{max})$ and $T(\varepsilon_{max})$ are the temperatures corresponding to ε_{max} and $0.9\varepsilon_{max}$.[1] The data are shown in Fig. 3(c), indicating a gradual growth of ΔT with x. This peak broadening usually has three possible origins: relaxorlike FE interaction, AFE interaction, or competitions between multifold interactions (e.g., the competition between the Ba^{2+}-doping-induced quadrupole ordering and Ca^{2-}doping-induced off-center dipole ordering). However, it is unlikely to observe a well-developed P-E loop for the FE relaxor state. For the high Ca-doping case, it is the AFE interaction responsible for the broad dielectric peak. To confirm this argument, we present the measured $\varepsilon(T)$ data for sample $x = 0.35$, as shown in Fig. 3(b). When the Curie-Weiss law $\varepsilon = C/(T - T_0)$, where C is the Curie constant and T_0 is the Curie temperature, is used to fit the high-T data, as shown in Fig. 3(d), one obtains $T_0 = -16.2$ K, a signature of the AFE interaction.[19]

Furthermore, the measured Raman spectra for this sample ($x = 0.35$) at $T = 50$, 75, 100, 150, 180, and 250 K, respectively, are shown in Fig. 3(f), noting the dielectric peak at ~160 K. Above 160 K, the Raman spectra present two broad bands at ~300 and 650 cm^{-1}, indicating mainly the second-order Raman mode. However, below 160 K, the strong first-order Raman peaks at 450 cm^{-1} (B_{1g} mode) and 538 cm^{-1} (AFE hard mode) confirm the AFE state.[20,21] This AFE state may result from the antiparallel displacements of Ti^{4+} and Sr^{2+}/Ca^{2+} ions along the [010] direction on the (001) plane of the ideal cubic perovskite.[14] The opposite polarizations of two sublattices must couple with each other, leading to the AFE transition in the high Ca-doped samples ($x > 0.25$).

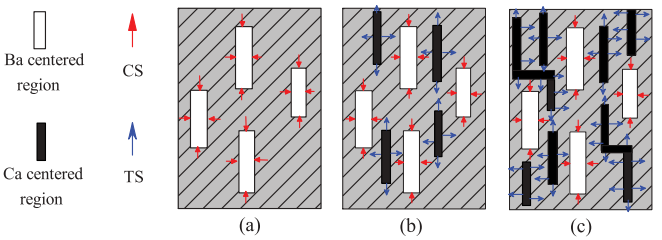

FIG. 4. (Color online) A sketch drawing of the FE domains (white bars) and/or AFE domains (black bars) in sample $x = 0$ (a), in the cooperative FE state (b), and in the AFE-dominant state at high x (c). The arrows indicate the stress onto the domains.

Based on the above discussion, one can now explain the observed unusual behaviors in the low-level Ca-doped samples ($x < 0.25$). For large ion doping (e.g., Ba^{2+}), those doped regions present a larger TF (e.g., $t = 1.07$) than STO and a quadrupole occupation, inducing elastic lattice strain. Owing to the high polarizability of the STO host lattice, the as-generated quadrupole ordering can polarize the doped regions and thus form FE-like polar domains. However, owing to the difference in TF and thus lattice size between the doped regions and the STO host lattice, the polar domain formation may encounter resistance from the serious compressive stress (CS) imposed by the STO host matrix, as shown in Fig. 4 by red arrows onto the white bars.[11,12] These quadrupole-ordered regions (white bars in Fig. 4) can be viewed as local and small FE domains that are randomly distributed. Under a high E, these domains realign themselves toward the direction of E, generating significant P_s. However, upon removal of E, the CS imposed on these domains will enforce them back to the original alignments. Therefore, the measured P_r and E_c must be very small although P_s can be large, which is the reason for the serious PR effect in sample $x = 0$.

On the other hand, for small ion doping (e.g., Ca^{2+}), those doped regions show a smaller TF (e.g., $t = 0.97$) than STO and thus allow off-center ion occupation. The as-generated off-center dipole ordering can lead to the formation of AFE-like polar domains, as shown by the black bars in Fig. 4. The size of these polar domains increases with decreasing temperature. More importantly, these regions are seriously tensioned with evident tensile stress (TS), because of the difference in the TF and thus lattice size between the STO host lattice and the doped regions. The random distribution of the two types of polar domains (quadrupole-ordered regions and the off-center dipole-ordered regions) thus allows the efficient coupling between them and an efficient release of both the CS and TS, leading to a gradual suppression of

the above-mentioned PR effect with increasing x. Given this release effect, a well-developed P-E loop with increasing P_r and E_c becomes reasonably expected. This corresponds to the enhanced FE region shown in Fig. 2, and it is this amazing cooperative behavior that makes the Ca doping enhance significantly the FE performance, as long as the doping level is not high.

With increasing x, besides the coupling effect highlighted above, which is preferred in terms of FE enhancement, the competition of the Ca-doping-induced AFE polar domains against the FE polar domains becomes serious. An overdoping of Ca^{2+}, on the one hand, induces additional TSs and thus breaks the optimized stress release, and, on the other hand, those local AFE polar domains becomes dominant and eventually transform the system into the AFE state, as schematically shown in Fig. 4(b). Therefore, a balance between the coupling and competition in terms of the FE and AFE orders can be maintained only for a proper Ca-doping range, in which the stresses are fully released while the FE state is dominant, as shown in Fig. 4(a).

Our experiments reveal an interesting phenomenon in Ba and Ca codoped STO, which is not available in the individual cases. The core physics lies in the coupling and competition between these two types of polar-ordering domains. Surely this phenomenon may not always occur. For example, for either Ba^{2+} or Ca^{2+} individual doping, if the doping level is high, macroscopic FE or AFE domains will be developed over the whole sample. At this stage, no more condition for stress generation is satisfied. Therefore, the phenomenon revealed in the present work represents a delicate combination of the multifold ingredients, which may thus shed light on the synthesis of FEs with attractive performance. Nevertheless, what should be indicated here is that we start from the dipole domain scenario as schematically shown in Fig. 4, while we do not have direct and visible evidence with the domains. One may be aware of the possibility of homogeneous mixing of Ba^{2+} and Ca^{2+} ions in the lattice level, and thus no presence of the above-mentioned FE and AFE domains. This awareness seems inconsistent with the observed fact and we argue that the proposed model here should apply.

In conclusion, we have investigated the coupling and competition between the quandrupole ordering and off-center dipole ordering, induced by Ba^{2+} and Ca^{2+} doping respectively, in polycrystalline SBCT. Owing to the mutual cooperative behavior, an unconventional and significantly enhanced FE property has been proven in properly Ca-doped SBCT. More interestingly, it is shown that the Ca doping results in the appearance of multipolarized states, from the enhanced FE state to the cooperative polarization state, and eventually to the AFE state.

This work was supported by the Natural Science Foundation of China (11074113, 50832002), the National Key Projects for Basic Researches of China (2009CB623303, 2011CB922101), and the Scientific Research Foundation of Civil Aviation University of China (2010QD01X).

*liujm@nju.edu.cn

[1] J. G. Bednorz and K. A. Müller, Phys. Rev. Lett. **52**, 2289 (1984).
[2] I. Katayama, H. Shimosato, D. S. Rana, I. Kawayama, M. Tonouchi, and M. Ashida, Appl. Phys. Lett. **93**, 132903 (2008).
[3] M. Itoh, R. Wang, Y. Inaguma, T. Yamaguchi, Y.-J. Shan, and T. Nakamura, Phys. Rev. Lett. **82**, 3540 (1999).
[4] A. I. Frenkel, D. Ehre, V. Lyahovitskaya, L. Kanner, E. Wachtel, and I. Lubomirsky, Phys. Rev. Lett. **99**, 215502 (2007).
[5] D. A. Tenne, A. Soukiassian, X. X. Xi, H. Choosuwan, R. Guo, and A. S. Bhalla, Phys. Rev. B **70**, 174302 (2004).
[6] D. E. Grupp and A. M. Goldman, Science **276**, 392 (1997).
[7] S. Nozawa, T. Iwazumi, and H. Osawa, Phys. Rev. B **72**, 121101(R) (2005).
[8] W. Kleemann and H. Schremmer, Phys. Rev. B **40**, 7428 (1989).
[9] V. V. Lemanov, E. P. Smirnova, P. P. Syrnikov, and E. A. Tarakanov, Phys. Rev. B **54**, 3151 (1996); V. V. Lemanov, Ferroelectrics **226**, 133 (1999).
[10] C. Ménoret, J. M. Kiat, B. Dkhil, M. Dunlop, H. Dammak, and O. Hernandez, Phys. Rev. B **65**, 224104 (2002).
[11] B. E. Vugmeister and M. D. Glinchuk, Rev. Mod. Phys. **62**, 993 (1990).
[12] G. A. Samara, J. Phys. Condens. Matter **15**, R367 (2003).
[13] S. K. Mishra and D. Pandey, Appl. Phys. Lett. **95**, 232910 (2009).
[14] R. Ranjan, D. Pandey, and N. P. Lalla, Phys. Rev. Lett. **84**, 3726 (2000).
[15] V. Porokhonskyy, A. Pashkin, V. Bovtun, J. Petzelt, M. Savinov, P. Samoukhina, T. Ostapchuk, J. Pokorny, M. Avdeev, A. Kholkin, and P. Vilarinho, Phys. Rev. B **69**, 144104 (2004).
[16] V. V. Shvartsman, S. Bedanta, P. Borisov, W. Kleemann, A. Tkach, and P. M. Vilarinho, Phys. Rev. Lett. **101**, 165704 (2008).
[17] T. Wei, Y. J. Guo, P. W. Wang, D. P. Yu, K. F. Wang, C. L. Lu, and J.-M. Liu, Appl. Phys. Lett. **92**, 172912 (2008).
[18] D. Fu, M. Itoh, S. Y. Koshihara, T. Kosugi, and S. Tsuneyuki, Phys. Rev. Lett. **100**, 227601 (2008); D. Fu, M. Itoh, and S. Koshihara, J. Phys. Condens. Matter **22**, 052204 (2010).
[19] R. Blinc and B. Zeks, *Soft Modes in Ferroelectrics and Antiferroelectrics* (North-Holland, Amsterdam, 1974).
[20] M. A. Carpenter, C. J. Howard, K. S. Knight, and Z. Zhang, J. Phys. Condens. Matter **18**, 10725 (2006).
[21] S. K. Mishra, R. Ranjan, D. Pandey, R. Ouillon, J.-P. Pinan-Lucarre, P. Ranson, and P. Pruzan, Phys. Rev. B **64**, 092302 (2001).